J. Korean Inst. Electr. Electron. Mater. Eng.
Vol. 36, No. 4, pp. 376-384 July 2023
DOI: https://doi.org/10.4313/JKEM.2023.36.4.8
ISSN 1226-7945(Print), 2288-3258(Online)

Regular Paper

Optimizing the Performance of Three-Dimensional Nitrogen-Doped Graphene Supercapacitors by Regulating the Nitrogen Doping Concentration

Zhaoyang Han[1] and Sang-Hee Son[2]

[1] Department of Electronic Engineering, Cheongju University, Cheongju 28503, Korea

[2] Department of System Semiconductor Engineering, Cheongju University, Cheongju 28503, Korea

(Received April 6, 2023; Revised April 20, 2023; Accepted April 24, 2023)

Abstract: Nitrogen-doped graphene was synthesized by a hydrothermal method using graphene oxide (GO) as the raw material, urea as the reducing agent and nitrogen as the dopant. The morphology, structure, composition and electrochemical properties of the samples are characterized by scanning electron microscopy (SEM), transmission electron microscopy (TEM), Fourier transform infrared (FTIR) spectroscopy, X-ray diffraction (XRD), X-ray photoelectron spectroscopy (XPS), nitrogen adsorption-desorption analysis, electrical conductivity and electrochemical tests. The results show that urea can effectively reduce GO and achieve nitrogen doping under the hydrothermal conditions. By adjusting the mass ratio of raw materials to dopants, the graphene with different nitrogen doping contents can be obtained; the nitrogen content range is from 5.28~6.08% (atomic fraction percentage).When the ratio of dopant to urea is 1:30, the nitrogen doping content reaches a maximum of 6.08%.The supercapacitor performance test shows that the nitrogen content prepared by the ratio of 6.08% is the best at 0.1 A • g^{-1}. The specific capacitance is 95.2 F • g^{-1}.

Keywords: Graphene, Nitrogen doping, Urea, Hydrothermal method, Supercapacitors

1. INTRODUCTION

As non-renewable resources like coal, oil, and natural gas continue to deplete and environmental pollution worsens, it becomes increasingly urgent to research and develop new energy storage devices that can provide renewable, green, and clean energy for human beings. Supercapacitors have emerged as a solution in this context, as they possess the characteristics of both traditional capacitors and secondary batteries [1]. Supercapacitors have the potential to outperform traditional capacitors in terms of specific energy, as well as secondary batteries in terms of specific power. They also offer a longer cycle life, making them an excellent energy storage device. As a result, supercapacitors have broad application prospects in various fields, including aerospace systems, communication engineering, computers, and microelectronic devices. The performance of supercapacitor electrode materials is a crucial factor that affects the performance of capacitors and the development of related technologies. It directly determines the overall performance of capacitors [2]. Therefore, the premise that supercapacitors can fulfill the growing demand for new energy sources relies on the development of new materials that exhibit outstanding performance while being environmentally friendly [3]. Graphene, a newly discovered carbon allotrope after fullerenes and carbon nanotubes, possesses unique

✉ **Sang-Hee Son; shson@cju.ac.kr**

atomic and electronic structures that give it extraordinary properties not found in traditional materials. These properties make it an ideal candidate for use as electrode materials in supercapacitors. Chemical modification techniques such as generating derivatives, surface functionalization, chemical modification, and chemical doping can effectively adjust the structure and properties of graphene. This leads to a wider range of functions and applications for graphene and related materials. In order to achieve chemical doping, nitrogen atoms can be utilized as electron donors to substitute graphene, as they have a similar atomic radius to carbon atoms. The resulting nitrogen-doped graphene exhibits superior properties compared to pure graphene. As a result, the process of nitrogen doping has become a popular topic in the field of graphene chemical modification research.

Several methods are currently available for nitrogen doping of graphene, including chemical vapor deposition (CVD), N_2 plasma treatment, arc discharge, high-energy electrothermal, and template methods [4-6]. The CVD method is the most commonly used technique for preparing nitrogen-doped graphene. Mr. Wei utilized this method to successfully produce nitrogen-doped graphene with fewer layers. He did this by using a silicon wafer substrate that was covered with a 25 nm thick copper film in a H_2-Ar mixed atmosphere with methane and ammonia as carbon and nitrogen sources [7]. Similarly, Mr. Jeong also obtained nitrogen-doped graphene through the N_2 plasma-enhanced chemical vapor deposition process [8]. The supercapacitor performance test shows that the specific capacitance of the material is as high as about 280 $F \cdot g^{-1}$, which is four times higher than that of pure graphene [9]. The CVD method involves a deposition reaction that uses a toxic gas source and leaves residual gas, requiring high reaction temperatures and specialized substrate materials and experimental equipment. These factors ultimately increase production costs [10]. In 2011, Xia's group proposed a simple, catalyst-free thermal annealing method, which can prepare graphene with high nitrogen doping content in large quantities: they selected low-cost industrial raw material melamine as the nitrogen source [11]. After grinding it with graphene oxide (GO), the nitrogen doping of graphene was realized by high temperature annealing in Ar atmosphere, and the synthesized material showed more advantageous electrocatalytic O_2 reduction activity than pure graphene [12]. Numerous methods exist for preparing nitrogen-doped graphene, with nitrogen-containing compounds such as ammonia, pyridine, acetonitrile, melamine, urea, and nitrogen plasma commonly used as nitrogen sources. Urea, in particular, is a reagent with high nitrogen content that is easily soluble in water, less toxic, environmentally friendly, and exhibits good reduction ability. In a study by Wakeland, graphene oxide was mixed with urea and heated to 600°C in an N_2 atmosphere to produce graphene with low residual oxygen content. Urea was used as both an expansion and reducing agent during the process [13]. Mou reported the use of thermal solid phase reaction in Ar atmosphere, at 600 and 700°C, the mixture of graphene oxide and urea obtained doped graphene with a nitrogen content of about 10% (Based on atomic fraction, the same goes for other parts of the article) [14]. In a study conducted by Fu's research group, doped graphene with a nitrogen content of up to 10.13% was obtained through a one-step hydrothermal process using GO and urea [15]. However, the process has some drawbacks such as high reaction temperature, long reaction time (180°C, 12 h), and large amount of urea, which ultimately increases the production cost and makes it challenging for subsequent treatment. In this paper, GO was utilized as the raw material while urea was used as both the reducing agent and nitrogen dopant. The hydrothermal reaction was conducted under mild experimental conditions at 160°C for 3 hours.

2. EXPERIMENT PART

2.1 Raw materials and reagents

In this study, graphene oxide (0.5 g) was obtained from Jiangsu Xianfeng Nanomaterials Technology Company. All other reagents, including urea, anhydrous ethanol, acetone, KOH, K_2S_2O8, P_2O_5, $KMnO_4$, HCl, H_2SO_4, and H_2O_2, were commercially available and analytically pure, and were produced by Sinopharm Chemical Reagent Company. Secondary deionized water was used in the experiments.

2.2 Preparation of nitrogen-doped graphene by hydrothermal method

15 mg graphene oxide was ultrasonically dispersed into 40 mL deionized water. To prevent the stacking of graphene oxide due to excessive water temperature, we replaced the

water in the supergenerator every 30 minutes during the ultrasonic process. ultrasound was used to mix urea into a transparent aqueous solution. The resulting solution was then loaded into a 50 mL polytetrafluoroethylene reactor and reacted at 160℃ for 3 hours. After cooling to room temperature, a black block solid was obtained. This solid was washed multiple times with deionized water and freeze-dried in a freeze dryer. In this study, the obtained samples were labeled as NG-X, where NG refers to nitrogen-doped graphene, and X represents the mass ratio of graphene oxide to urea (1:10, 1:30, and 1:50). As a comparative experiment, 15 mg of graphene oxide ultrasonic dispersion was added directly to a polytetrafluoroethylene reactor without urea, and the hydrothermal reaction was performed at 160℃ for 3 hours. The product obtained from this process was labeled as RGO, which stands for reduced graphene oxide.

Fig. 1. A three-dimensional nitrogen-doped graphene placement map on petals and stamens.

3. RESULTS AND DISCUSSION

3.1 Characterization of physical and chemical properties

As shown in Fig. 1, the nitrogen-doped graphene sponge we prepared has a certain shape after the hydrothermal reaction. The shape is kept unchanged by freeze-drying. The nitrogen-doped graphene sponge is lighter. The nitrogen-doped graphene sponge is placed on the petals and stamens. Because of the lighter weight, the nitrogen-doped graphene sponge can be easily placed. The petals and stamens can withstand the quality of the graphene sponge. By adjusting the hydrothermal reaction temperature, time and urea content, the other characteristics of the sponge can be changed and the specific surface area of the nitrogen-doped graphene sponge can be improved [16]. Here we do not do too much research.

As shown in Fig. 2, the SEM images of nitrogen-doped graphene prepared at different ratios are shown. From the figure, we can see that the graphene sheets are disorderly staggered and interconnected to form a three-dimensional porous network structure. The gap of the network structure is about a few microns. This porous three-dimensional structure has a large surface area, which can make the electrode surface fully contact with the electrolyte, so as to achieve a good ability to store charge, and provide a large place for the formation of double-layer capacitance required for supercapacitors [17].

Figure 3 shows the TEM image of NG-30. From Fig. 3, it can be seen that the nitrogen-doped graphene presents a wrinkled, transparent and disordered thin yarn shape, and the thicker part is the multilayer structure formed by stacking between different layers. This wrinkle around the yarn is attributed to the defectstructure formed by the doping of nitrogen atoms in urea during the hydrothermal process, the

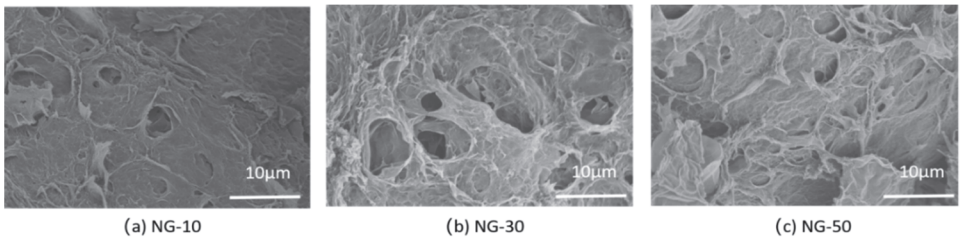

Fig. 2. SEM images of NG-X (X=10, 30, and 50).

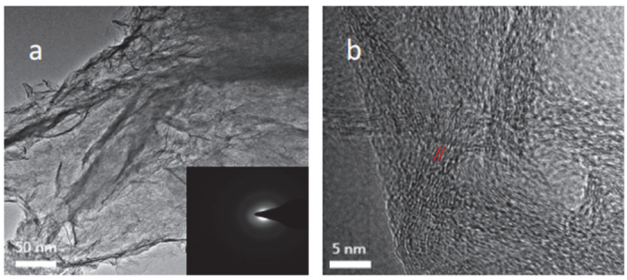

Fig. 3. TEM image of NG-30.

defect structure can be seen by high-resolution transmission electron microscopy. As shown in Fig. 3, it is a selected area electron diffraction pattern of NG-30. The diffraction ring is clearly visible, but the hexagonal lattice diffraction bright spot is not obvious, indicating that the original long-range order of graphene after nitrogen atom doping has disappeared [18].

Figure 4 is the elemental analysis diagram of NG-30. It can be seen from Fig. 4(b) that NG-30 contains C, N, O, and other elements [19]. According to the color, it can be judged that the carbon content is larger and the nitrogen content is smaller. The specific content will be quantitatively tested in the next XPS test.

Figure 5 is the Raman spectra of nitrogen-doped graphene prepared at different ratios. It can be intuitively seen from the figure that the intensity of Raman peaks shown by different proportions of samples is different, but the difference is not large. The strongest peak is RGO [20]. Upon introduction of nitrogen atoms, the original Raman peaks have exhibited varying degrees of decrease, with the GO (002) diffraction peak at 2=11.8° NG-30 displaying the lowest intensity. It is currently speculated that this decrease may be attributed to a high nitrogen doping content in NG-30. Further testing is required to verify this hypothesis.

Figure 6 is XRD patterns of RGO, NG-10, NG-30, and NG-50. From the diagram, it can be seen that the RGO (002) diffraction peak is at 2θ=24.3°, corresponding to d=0.366 mm. The (002) is diffraction peak of nitrogen-doped graphene is slightly different from the RGO (002) diffraction peak [21]. The (002) diffraction peak of nitrogen-doped graphene at 24.6°, corresponding to d=0.362 mm, indicating that during the

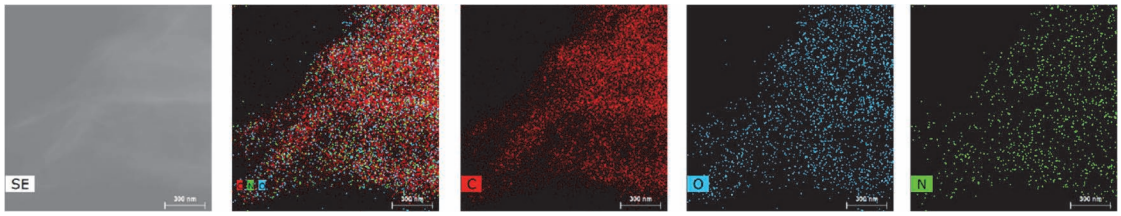

Fig. 4. TEM elemental mapping images analysis of NG-30.

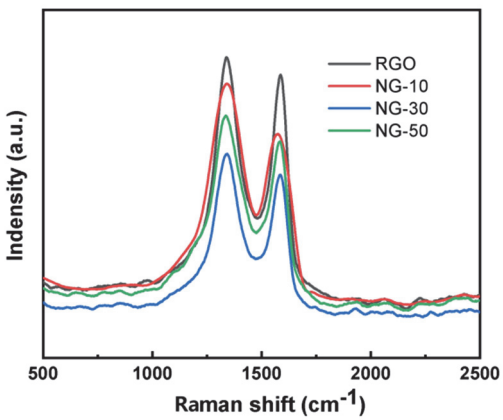

Fig. 5. Raman spectra of RGO, NG-10, NG-30, and NG-50.

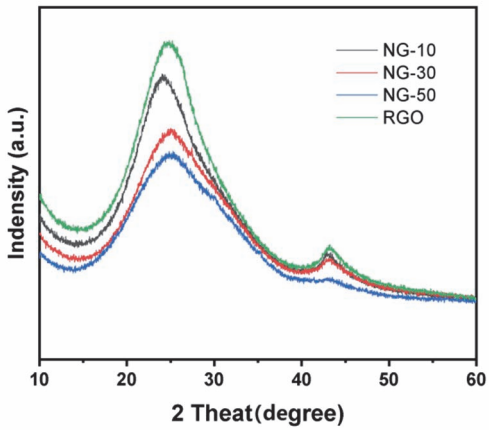

Fig. 6. XRD patterns of RGO, NG-10, NG-30, and NG-50.

process, the addition of urea makes the degree of graphene reduction deeper [22]. At the same time, the graphite lattice structure has also been restored to a certain extent after the hydrothermal reaction.

To investigate the impact of urea on the reduction degree of graphene oxide and the role of nitrogen doping in the hydrothermal process, we conducted quantitative and qualitative analysis of the samples using XPS. Figure 7(a) shows the XPS full spectrum of NG-10, NG-30, and NG-50. The intensity of the C1s peak increases while the intensity of the O1s peak decreases during the hydrothermal reaction, indicating the recovery of C in the sp2 region. Quantitative analysis reveals that the atomic ratios of C:O are 5.31, 8.53, 9.23, and 8.25 for RGO, NG-10, NG-30, and NG-50, respectively. It can be seen that the ratio of C:O gradually increases with the addition of urea.

Compared with RGO, the ratio of C:O becomes larger after nitrogen doping [23]. At the same time, from the data point of view, the N1s peak was added, indicating that we successfully doped the N element. The nitrogen content of NG-10, NG-30, and NG-50 was 5.28%, 6.08%, and 5.67% (atomic number percentage), respectively, indicating that the nitrogen content of NG-30 sample was the highest, which was consistent with the above test conclusions. Therefore, when the ratio of graphene to urea was 1:30, urea could fully doped nitrogen into graphene, and the ratio of graphene to urea was 1:30. At the same time, we made XPS fitting for NG-30 samples. By fitting the C element, we found that the C element in NG-30 was composed of C-O/C-O-C (286.9 eV), C=O (288.0 eV), O-C=O (289.1 eV), C=C (284.6 eV) and C-N (285.9 eV) peaks [24]. By fitting the N1s peaks, it is found that the N atoms replace the C atoms in the graphene lattice in the form of 'pyridinic N' (398.2 eV), 'pyrrolic N' (399.5 eV), and 'graphitic N' (401.5 eV) [24].

3.2 Supercapacitor performance test

In order to test the supercapacitor performance of nitrogen-doped graphene materials, it is necessary to grind the active material materials into powder to prepare electrode samples, and the prepared electrodes are tested by a three-electrode system. The preparation method of the electrode is as follows:

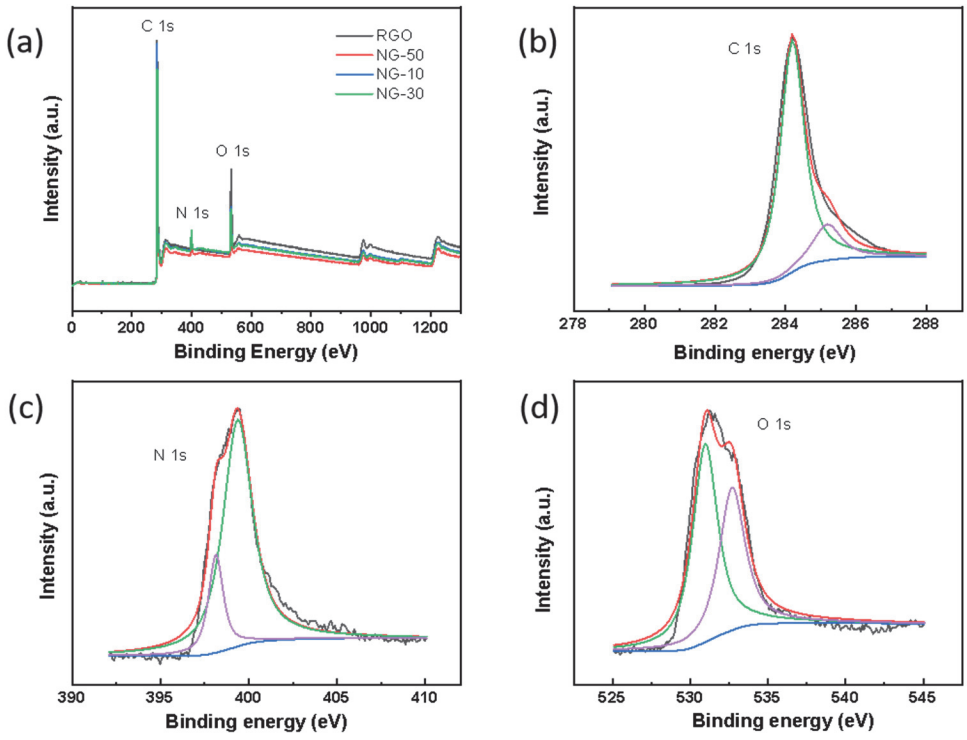

Fig. 7. (a) XPS of different samples is universal and (b-d) XPS peak fitting diagram of NG-30.

First, cut a piece of 1×3 cm^2 nickel foam, Rinse with dilute hydrochloric acid, anhydrous ethanol, and deionized water for 5 minutes, and then dry in an drying cabinet, the weight of dried nickel is recorded as M1. Secondly, the prepared active material powder, polyvinylidene fluoride and acetylene black are configured according to the mass ratio of 8:1:1. After the configuration is fully ground, NMP is added and stirred evenly. Continue grinding, the amount of NMP added should be based on the viscosity of the sample until the sample is a mixed slurry material suitable for coating. Finally, the slurry material after grinding was evenly applied to 1×3 cm^2 nickel foam at one end of 1×1 cm^2. After coating, the nickel foam was put into the oven at 80℃ for 12 h. After drying, the side of the sample was painted inward, and the side was folded and placed in the tableting machine. The pressure was 3~5 Mpa. After the tableting was finished, it was put into the oven for overnight drying, and the electrode material was finally obtained.

The CV cyclic voltammetry curves of RGO, NG-10, NG-30, and NG-50 at 10, 30, 50, and 100 $mV \cdot s^{-1}$ scan rates are shown in Fig. 8, respectively. Through the CV curve, we can see that the CV cycle curve of RGO has obvious redox peaks. This is because during the hydrothermal reaction, graphene oxide undergoes a redox reaction, but the symmetry is not good enough and does not have good reversibility [25]. From the cyclic voltammetry curves of NG-10, NG-30, and NG-50 in the graph, it can be seen that the image shows good symmetry and has obvious redox peaks. From the area point of view, the area enclosed by the CV curve of the nitrogen-doped sample is significantly larger than the CV cycle curve of RGO, indicating that the introduction of nitrogen doping reduces the agglomeration of graphene, and presents a three-dimensional porous structure. The larger specific surface area can have sufficient contact with the electrolyte, and the electrolyte in the supercapacitor can fully penetrate into the electrode material [26]. At the same time, we found that different urea contents lead to different degrees of nitrogen doping. The CV curve area of three nitrogen-doped graphene samples with different urea contents also has slight differences. Among them, the CV curve area of NG-30 sample is the largest, followed by NG-10 and NG-50, but the difference is not large, indicating that the doping of nitrogen can improve the ability of graphene to store charge, and the content of nitrogen directly affects the ability of supercapacitor system to store charge [27].

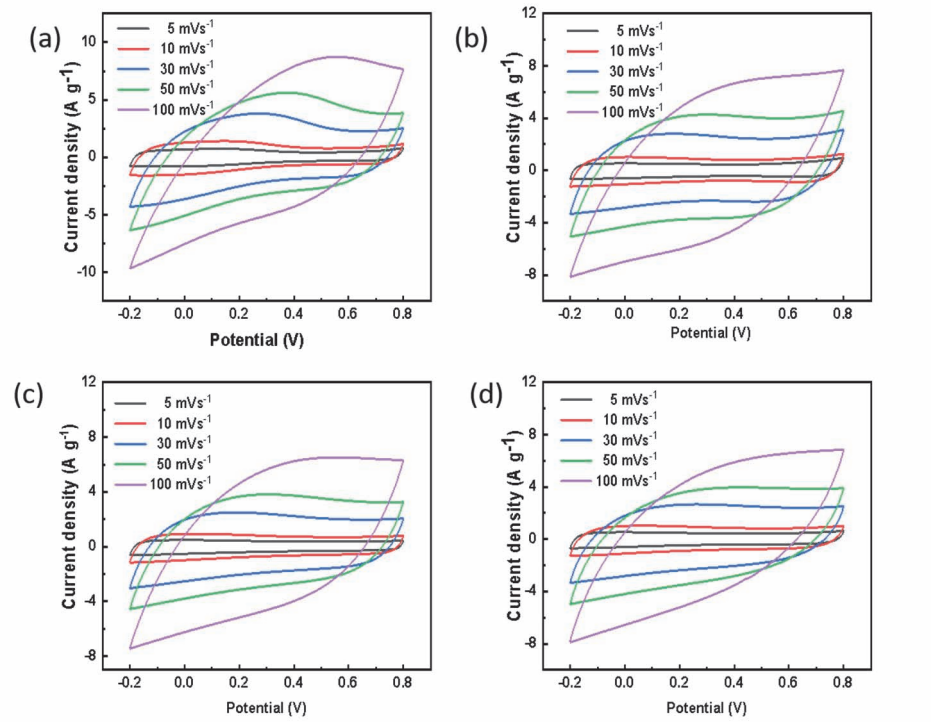

Fig. 8. CV curves at the different scan rates (5~100 $mV \cdot s^{-1}$). (a) RGO, (b) NG-10, (c) NG-30, and (d) NG-50.

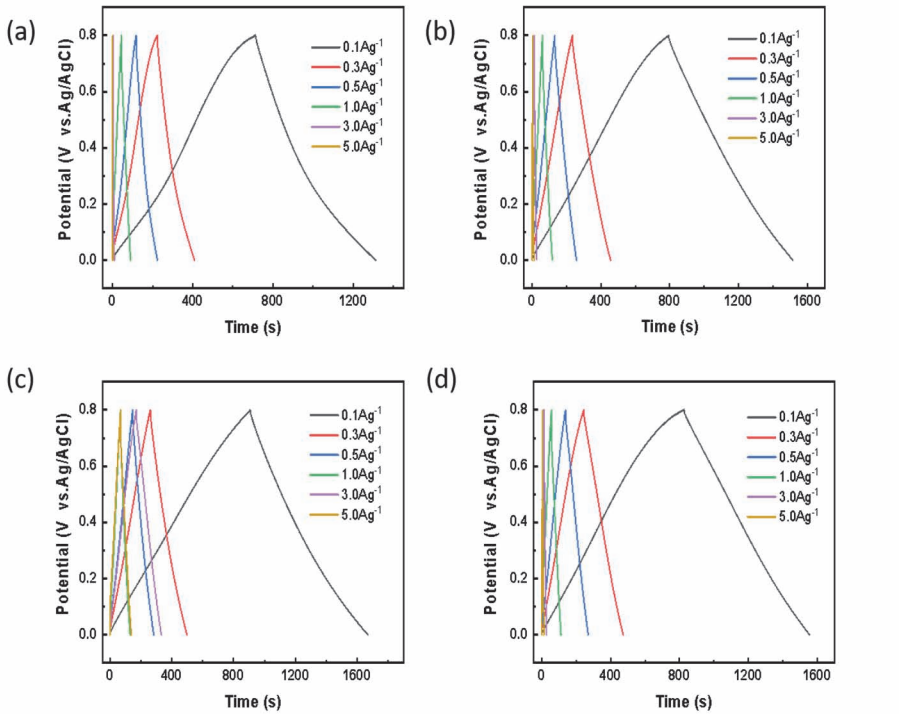

Fig. 9. Constant current charge and discharge curves of RGO and NG-X (X =10, 30, and 50)

The galvanostatic charge-discharge curves of RGO, NG-10, NG-30, and NG-50 at current densities of 0.1, 0.3, 0.5, 1, 3, and 5 A·g^{-1} are shown in Fig. 9, respectively. All curves show a similar isosceles triangle curve, but not completely symmetrical, which may be due to the Faraday pseudocapacitance effect caused by the doped nitrogen atoms and some oxygen-containing functional groups in the material. From the diagram, it can be seen that the constant current charge-discharge curve after nitrogen doping is better than that of RGO in symmetry. At a current density of 0.1 A·g^{-1}, the charge-discharge time of nitrogen-doped samples is significantly longer than that of RGO, indicating that the nitrogen-doped samples have stronger charge storage capacity, which is consistent with our CV cycle curve results. According to the charge-discharge time of different samples at a current density of 0.1 A·g^{-1}, it can be calculated. The capacitances of RGO, NG-10, NG-30, and NG-50 are 74.8 F·g^{-1}, 90 F·g^{-1}, 95.2 F·g^{-1}, and 92 F·g^{-1}, respectively. The maximum capacitance is NG-30, because the nitrogen content of NG-30 is high, and the porous structure increases the specific surface area and can better store charge [28].

Figure 10 displays the capacitance values of RGO, NG-10, NG-30, and NG-50 at current densities ranging from 0.1 to 5 A·g-1. The curve illustrates that as the current density increases, the capacitance value of RGO decreases at a faster rate compared to the other materials. Additionally, RGO is unable to maintain a high charge storage capacity at high current densities. The capacitance reduction trend of nitrogen-doped samples is not significant with increasing current density, indicating good capacitance retention ability. Notably, NG-30

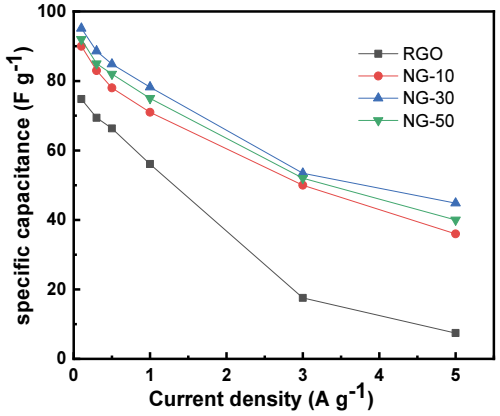

Fig. 10. The capacitance diagrams of RGO and NG-X (X=10, 30, and 50) at different current densities are shown.

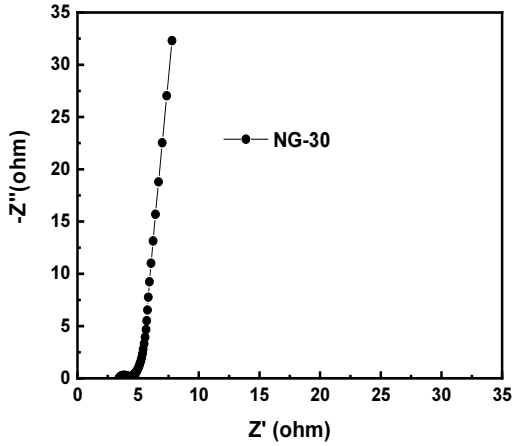

Fig. 11. AC impedance diagram of NG-30.

exhibits favorable capacitance value and retention rate, making it a promising electrode material for supercapacitors [29].

To further evaluate the effectiveness of NG-30 samples as supercapacitors, we conducted AC impedance tests on them. The tests were carried out using a frequency range of 100 kHz to 0.01 Hz. As shown in Fig. 11, the AC impedance curve of NG-30 is almost vertical in the low-frequency region, and a clear semicircle appears in the high-frequency region. This occurrence is attributed to the influence of Faraday resistance [30]. The results of the study indicate that NG-30, a type of nitrogen-doped graphene with a nitrogen content ranging from 5.28% to 6.08%, has a lower resistance and is a suitable material for supercapacitors. The synthesis of NG-30 was successfully achieved through a mild experimental process lasting 3 hours at 160°C.

4. CONCLUSION

Graphene with varying levels of nitrogen doping was synthesized under hydrothermal conditions of 160°C and 3 hours by adjusting the mass ratio of raw material to dopant. The raw material used was GO, while urea served as the reducing agent and nitrogen dopant. XPS analysis showed that the nitrogen content of different materials was also different (5.28~6.08%), and the nitrogen atoms doped into the graphene lattice existed in three forms: ‘pyridinic N’, ‘pyrrolic N’, and ‘graphitic N’. The relative content of the three is also slightly different in different materials [31]. According to electrochemical tests, the nitrogen-doped graphene with a nitrogen content of 7.50% exhibits the most superior supercapacitor performance, with a specific capacitance of 95.2 $F \cdot g^{-1}$. Nitrogen-doped graphene was successfully synthesized using mild experimental conditions resulting in a material with a typical mesoporous structure. This structure was attributed to the increased conductivity of the raw material GO and the nitrogen atoms that were doped into the graphene lattice.

ORCID

Sang-Hee Son http://orcid.org/0000-0003-4392-066X

ACKNOWLEDGEMENT

This paper was supported by Korea Institute for Advancement of Technology (KIAT) grant funded by the Korea Government (MOTIE) (P0017011, HRD Program for Industrial Innovation).

REFERENCES

[1] Z. Han and S. H. Son, *J. Korean Inst. Electr. Electron. Mater. Eng.*, **36**, 175 (2023). [DOI: https://doi.org/10.4313/JKEM.2023.36.2.11]

[2] H. R. Yu, *J. Korean Inst. Electr. Electron. Mater. Eng.*, **31**, 112 (2018). [DOI: https://doi.org/10.4313/JKEM.2018.31.2.112]

[3] S. Kim, *J. Korean Inst. Electr. Electron. Mater. Eng.*, **33**, 360 (2020). [DOI: https://doi.org/10.4313/JKEM.2020.33.5.360]

[4] Y. Wang, W. Zhou, Q. Kang, J. Chen, Y. Li, X. Feng, D. Wang, Y. Ma, and W. Huang, *ACS Appl. Mater. Interfaces*, **10**, 27001 (2018). [DOI: https://doi.org/10.1021/acsami.8b06710]

[5] R. S. Kalubarme, H. S. Jadhav, and C. J. Park, *Electrochim. Acta*, **87**, 457 (2013). [DOI: https://doi.org/10.1016/j.electacta.2012.09.081]

[6] Y. Wang, W. Huo, X. Yuan, and Y. Zhang, *Acta Phys.-Chim. Sin.*, **36**, 1904007 (2020). [DOI: https://doi.org/10.3866/PKU.WHXB201904007]

[7] X. L. Bai, Y. L. Gao, Z. Y. Gao, J. Y. Ma, X. L. Tong, H. B. Sun, and J. A. Wang, *Appl. Phys. Lett.*, **117**, 183901 (2020). [DOI: https://doi.org/10.1063/5.0018708]

[8] S. B. Hong, J. M. Jeong, H. G. Kang, D. Seo, Y. Cha, H. Jeon, G. Y. Lee, M. Irshad, D. H. Kim, S. Y. Hwang, J. W. Kim, and B. G. Choi, *ACS Appl. Mater. Interfaces*, **10**, 35250 (2018). [DOI: https://doi.org/10.1021/acsami.8b12894]

[9] S. H. Partil, A. P. Gaikwad, B. J. Waghmode, S. D. Sathaye, and K. R. Patil, *New. J. Chem.*, **44**, 6853 (2020). [DOI: https://doi.org/10.1039/C9NJ05898B]

[10] C. Zhu, X. Dong, X. Mei, M. Gao, K. Wang, and D. Zhao, *J. Mater. Sci.*, **55**, 17108 (2020). [DOI: https://doi.org/10.1007/s10853-020-05212-2]

[11] G. Li, Y. Lu, C. Lu, M. Zhu, C. Zhai, Y. Du, and P. Yang, *J. Hazard. Mater.*, **294**, 201 (2015). [DOI: https://doi.org/10.1016/j.jhazmat.2015.03.045]

[12] B. Li, G. Rong, Y. Xie, L. Huang, and C. Feng, *Inorg. Chem.*, **45**, 6404 (2006). [DOI: https://doi.org/10.1021/ic0606274]

[13] Y. P. Li and Y. Z. Hao, *Acta Phys.-Chim. Sin.*, **26**, 3365 (2010). [DOI: https://doi.org/10.3866/PKU.WHXB20101205]

[14] X. L. Bai, X. Tong, Y. Gao, W. Zhu, C. Fu, J. Ma, T. Tan, C. Wang, Y. Luo, and H. Sun, *Electrochim. Acta*, **281**, 525 (2018). [DOI: https://doi.org/10.1016/j.electacta.2018.06.003]

[15] J. Yan, Z. Fan, T. Wei, W. Qian, M. Zhang, and F. Wei, *Carbon*, **48**, 3825 (2010). [DOI: https://doi.org/10.1016/j.carbon.2010.06.047]

[16] G. Zhu, Z. He, J. Chen, J. Zhao, X. Feng, Y. Ma, Q. Fan, L. Wang, and W. Huang, *Nanoscale*, **6**, 1079 (2014). [DOI: https://doi.org/10.1039/c3nr04495e]

[17] L. S. Panchokarla, K. S. Subrahmanyam, S. K. Saha, A. Govindaraj, H. R. Krisnamurthy, U. V. Waghmare, and C.N.R. Rao, *Adv. Mater.*, **21**, 4726 (2009). [DOI: https://doi.org/10.1002/adma.200901285]

[18] X. Wang, X. Li, L. Zhang, Y. Yoon, P. K. Weber, H. Wang, J. Guo, and H. J. Dai, *Science*, **324**, 768 (2009). [DOI: https://doi.org/10.1126/science.1170335]

[19] B. Guo, Q. Liu, E. Chen, H. Zhu, L. Fang, and J. R. Gong, *Nano Lett.*, **10**, 4975 (2010). [DOI: https://doi.org/10.1021/nl103079j]

[20] Z. H. Sheng, L. Shao, J. J. Chen, W. J. Bao, F. B. Wang, and X. H. Xia, *ACS Nano*, **5**, 4350 (2011). [DOI: https://doi.org/10.1021/nn103584t]

[21] X. Li, H. Wang, J. T. Robinson, H. Sanchez, G. Diankov, and H. Dai, *J. Am. Chem. Soc.*, **131**, 15939 (2009). [DOI: https://doi.org/10.1021/ja907098f]

[22] Z. Jin, J. Yao, C. Kittrell, and J. M. Tour, *ACS Nano*, **5**, 4112 (2011). [DOI: https://doi.org/10.1021/nn200766e]

[23] A.L.M. Reddy, A. Srivastava, S. R. Gowda, H. Gullapalli, M. Dubey, and P. M. Ajayan, *ACS Nano*, **4**, 6337 (2010). [DOI: https://doi.org/10.1021/nn101926g]

[24] W. Qian, X. Cui, R. Hao, Y. Hou, and Z. Zhang, *ACS Appl. Mater. Interfaces*, **3**, 2259 (2011). [DOI: https://doi.org/10.1021/am200479d]

[25] Z. Mou, X. Chen, Y. Du, X. Wang, P. Yang, and S. Wang, *Appl. Surf. Sci.*, **258**, 1704 (2011). [DOI: https://doi.org/10.1016/j.apsusc.2011.10.019]

[26] S. Wakeland, R. Martinez, J. K. Grey, and C. C. Luhrs, *Carbon*, **48**, 3463 (2010). [DOI: https://doi.org/10.1016/j.carbon.2010.05.043]

[27] N. I. Kovtyukhova, P. J. Ollivier, B. R. Martin, T. E. Mallouk, S. A. Chizhik, E. V. Buzaneva, and A. D. Gorchinskiy, *Chem. Mater.*, **11**, 771 (1999). [DOI: https://doi.org/10.1021/cm981085u]

[28] W. S. Hummers and R. E. Offeman, *J. Am. Chem. Soc.*, **80**, 1339 (1958). [DOI: https://doi.org/10.1021/ja01539a017]

[29] C. Hontoria-Lucas, A. J. López-Peinado, J. de D. López-González, M. L. Rojas-Cervantes, and R. M. Martín-Aranda, *Carbon*, **33**, 1585 (1995). [DOI: https://doi.org/10.1016/0008-6223(95)00120-3]

[30] H. L. Guo, X. F. Wang, Q. Y. Qian, F. B. Wang, and X. H. Xia, *ACS Nano*, **3**, 2653 (2009). [DOI: https://doi.org/10.1021/nn900227d]

[31] Z. H. Liu, Z. M. Wang, X. Yang, and K. Ooi, *Langmuir*, **18**, 4926 (2002). [DOI: https://doi.org/10.1021/la011677i]